



# Enhanced hierarchical symbolic sample entropy: Efficient tool for fault diagnosis of rotating machinery

Shun Wang<sup>1</sup>, Yongbo Li<sup>1</sup> , Shubin Si<sup>2</sup> and Khandaker Noman<sup>1</sup>

## Abstract

Intelligent fault diagnosis of rotating machinery is a key topic for industrial equipment maintenance and fault prevention. In this study, an intelligent diagnosis approach of rotating machinery via enhanced hierarchical symbolic sample entropy (EHSSE) is proposed. Firstly, a novel indicator termed symbolic sample entropy (SSE) is proposed for complexity measure and representation of fault information. By using symbolic dynamic filtering, the raw continuous time-series will be discretized into symbolic data, and analysis of symbolic data is less sensitive to measurement noise, resulting in superior robustness. Secondly, SSE is combined with enhanced hierarchical analysis to further extract fault characteristics hidden in both low- and high-frequency components. To study the performance of SSE and EHSSE, multiple simulated signals and experimental studies are constructed and three widely used entropy methods are employed to present a comprehensive comparison. The comparison results show that EHSSE performs best in diagnosing various faults of planetary gearbox and rotor system with highest identification accuracy compared with other entropy-based approaches.

## Keywords

Sample entropy, symbolization, rotating machinery, hierarchical analysis, fault diagnosis, feature extraction

## Introduction

The rotating machinery has been widely utilized in mechanical equipment as an important part of mechanical transmission system.<sup>1,2</sup> However, during the actual operations, the key components of rotating machinery such as gear, bearing, and rotor are particularly prone to damage due to harsh working environments. Hence, the health state monitoring and fault diagnosis for rotating machinery has important practical significance in prevention of catastrophic failure and ensure reliable operation of industrial equipment.<sup>3–5</sup>

In past decades, on account of the health state monitoring and fault diagnosis, numerous investigations have been done on dynamic modeling, vibration signal processing, and intelligent fault diagnosis.<sup>6</sup> By means of modeling, several fault states like pitting, crack, missing, and wear, can be modeled. These models of rotating machinery may be conducive to understand the response behaviors of mechanical system,<sup>7,8</sup> thus they can provide valuable help for fault detection and diagnosis.<sup>9,10</sup> Moreover, the signal processing methods have been studied. Among signal processing methods, extracting suitable features and recognizing related patterns play a significant role for machine health monitoring.

In recent years, for quantitative analysis of system dynamics, researchers have proposed various signal complexity or orderliness indicators, especially the entropy-based tools.<sup>11</sup> The most widely used entropy-based methods mainly include approximate entropy (AE),<sup>12</sup> sample entropy (SE),<sup>11</sup> permutation entropy (PE),<sup>13</sup> symbolic dynamic entropy (SDE),<sup>14</sup> dispersion entropy,<sup>15</sup> fuzzy entropy (FE),<sup>16</sup> and multiscale-based entropy methods.<sup>17</sup> The above entropy indicators have been widely used in the diagnosis of different types of faults for bearing, planetary gearbox and other industrial equipment.<sup>18</sup>

For example, Yan et al. introduced AE to accomplish fault information extraction of rotating machinery.<sup>19</sup> multiscale sample entropy (MSE)-based features

<sup>1</sup>School of Aeronautics, Northwestern Polytechnical University, Xi'an, Shanxi, China

<sup>2</sup>School of Mechanics and Engineering, Northwestern Polytechnical University, Xi'an, Shanxi, China

## Corresponding author:

Yongbo Li, School of Aeronautics, Northwestern Polytechnical University, No. 127, Youyi Road(West), Beilin, Xi'an, Shanxi 710072, China.

Email: [yongbo@nwpu.edu.cn](mailto:yongbo@nwpu.edu.cn)

were conducted and utilized for the fault information representation of rolling bearings by Zhang et al.<sup>20</sup> Compared with SE, FE has a better performance because of the introduction of fuzzy function. As Zheng et al.<sup>21,22</sup> reported, FE can be highly sensitive to the dynamical change; thus FE can get a good performance in the health state monitoring of equipment. Moreover, Cheng et al. proposed a fault diagnosis method for planetary gear via fusion of ensemble empirical mode decomposition (EEMD)-based entropy feature.<sup>23</sup> multiscale permutation entropy (MPE) was used for the fault feature extraction of rolling bearing signals by Li et al.<sup>24</sup> Further, Li et al.<sup>14</sup> proposed multiscale SDE for the fault diagnosis of planetary gearbox, in which symbolic dynamic filtering (SDF) and state transition probability are introduced and combined with PE. Simulation and experimental case studies have verified that SDE obtains better performance and faster computation efficiency than SE and PE. Xu et al.<sup>25</sup> combined empirical mode decomposition (EMD) with symbolic entropy and proposed a fault flowchart for the diagnosis of bearing. Recently, multiscale fuzzy entropy-based on Euclidean distance was proposed,<sup>26</sup> which measures the similarity by the Euclidean distance.

Multiscale-based entropy methods, with a powerful ability for feature representation, has made vast inroads into the field of healthy condition monitoring of machines. However, the existing multiscale entropy methods still have two large obstacles in feature extraction: high-frequency information loss and poor robustness to disturbances and noises. First, the traditional coarse-graining multiscale analysis aims to obtain different scale series via averaging operation; however, the average operation is similar to smoothing the raw signal, which discards the information embedded in high-frequency component of signals. Second, in real-world data, the collected signals are distorted by disturbances and noises. Direct usage of the entropy without the noise reduction will seriously affect the accuracy of complexity estimation.

Therefore, the enhanced hierarchical symbolic sample entropy (EHSSE) method is proposed to handle the above problems. On the one hand, SDF is introduced to reduce the noise-related fluctuations and increase the robustness under low-signal to noise ratio (SNR) environment. By using SDF, the raw time-series will be discretized into symbolic data, so that the noise-related components will be reduced. On the other hand, to capture the fault characteristics from both high-frequency and low-frequency components, the enhanced hierarchical analysis strategy is proposed, which uses modified moving-averaging and moving-difference process to generate the multiple series for comprehensive feature extraction. Aside from that, a novel fault diagnosis

flowchart via EHSSE algorithm is proposed to accomplish fault type identification and diagnosis of rotating machinery. To confirm the effectiveness, two experimental case studies are constructed and three widely used methods are employed to present a comprehensive comparison. It has been shown that the proposed EHSSE performs better for the fault type identification and obtains the highest classification accuracy in comparison to widely used multiscale entropy-based methods. Overall, the proposed EHSSE method provides promising solution for achieving fault diagnosis with noise reduction and weak fault information extraction.

The remainder of this article is organized as follows. The concepts and calculation process of SSE and EHSSE methods are first introduced in “Method.” In “Simulation evaluation,” several simulation tests are designed and conducted to demonstrate the superiority of the proposed method. “Flowchart of proposed intelligent fault diagnosis method” describes the main steps of EHSSE-based diagnosis flowchart for rotating machinery. In “Case studies,” performance of the proposed method for recognizing fault state is shown by two case studies of rotating machinery. Lastly, in “Conclusions,” we conclude this article.

## Method

### Symbolic sample entropy

SSE employs a two-step procedure to enhance the ability in computation efficiency and robustness. First, the SDF approach is used for denoising purpose and conversion of the signal to the symbol sequence. Secondly, the variant form of SE is calculated based on symbolic sequences to measure the complexity and characterize the information of signals.

For a time-series  $S = \{s_1, \dots, s_i, \dots, s_N\}$  with length  $N$ , the detailed steps of proposed SSE are as follows.

**Step 1** Convert the time-series  $S$  into symbolic sequence  $y = \{y_1, y_2, \dots, y_N\}$  with  $\varepsilon$  numerical symbols. With the help of maximum entropy partitioning,<sup>27</sup> a discrete space is generated from a continuous state space, and subsequently the symbol sequence is obtained.

**Step 2** According to Taken’s Embedding theorem, construct embedding vectors with dimension  $m$ , which takes the form of equation (1).

$$s_i^m = \{y_i, y_{i+1}, \dots, y_{i+m-1}\}, \quad 1 \leq i \leq N - m \quad (1)$$

**Step 3** If two symbol vectors  $s_i^m$  and  $s_j^m$  are equal,  $i \neq j$ ,  $(s_i^m, s_j^m)$  is called as an  $m$ -dimensional matched vector pair. Here,  $\text{num}^m$  is obtained to indicate the total number of matched vector pairs under dimension  $m$ .

**Step 4** Repeat Steps (1)–(3) under dimension  $m+1$ , and then  $\text{num}^{m+1}$  can be used for indicating the vector pair number under dimension  $m+1$ .

**Step 5** Compute SSE value by the logarithm of the ratio of  $\text{num}^{m+1}$  to  $\text{num}^m$ , that is

$$\text{SSE} = -\ln \frac{\text{num}^{m+1}}{\text{num}^m} \quad (2)$$

### Enhanced hierarchical symbolic sample entropy

The entropy that describes the characteristics over a single scale contains poor fault information. To improve the feature representation capacity of entropy, enhanced hierarchical analysis is carried out in this subsection and then EHSSE is proposed. Hierarchical analysis was proposed by Jiang et al.,<sup>28</sup> which can evaluate the complexity from both low- and high-frequency components. Nonetheless, the traditional hierarchical procedure will reduce the length of sequence with the increase of hierarchical layer  $k$ , thus losing the statistical reliability. To overcome this shortcoming, EHSSE is introduced, where multiple series are generated from a single time-series by using modified moving-averaging and moving-difference process and then processed individually by using SSE. The length of sequence will not basically decrease with the increase of hierarchical layer  $k$  so that EHSSE performs better in stability comparing with conventional multiscale analysis and hierarchical analysis. Meanwhile, the proposed EHSSE gets rid of the requirement of data length  $N=2^n$  in the conventional hierarchical procedure. The detailed calculation steps are as follows.

**Step 1** Define averaging operator  $Q_0$  and difference operator  $Q_1$ . For a given a time-series  $X\{x(1), x(2), \dots, x(i), \dots, x(N)\}$ , the operators can be expressed as follows:

$$Q_0(x) = \frac{x(i) + x(i+1)}{2} \quad i = 1, 2, \dots, N-1 \quad (3)$$

$$Q_1(x) = \frac{x(i) - x(i+1)}{2} \quad i = 1, 2, \dots, N-1 \quad (4)$$

where the averaging operator  $Q_0$  and difference operator  $Q_1$  represent the low- and high-frequency information of time-series, respectively.

**Step 2** Illustrate the operators  $Q_j$  ( $j=0$  or  $1$ ) for the  $k$ -th layer using a matrix as follows:

$$Q_j^k = \begin{bmatrix} \frac{1}{2} & \frac{(-1)^j}{2} & 0 & \dots & 0 & 0 \\ 0 & \frac{1}{2} & \frac{(-1)^j}{2} & \dots & 0 & 0 \\ 0 & 0 & \frac{1}{2} & \dots & 0 & 0 \\ \vdots & \vdots & \vdots & \ddots & \vdots & \vdots \\ 0 & 0 & 0 & \dots & \frac{1}{2} & \frac{(-1)^j}{2} \end{bmatrix}_{(N-1) \times N} \quad (5)$$

**Step 3** The  $e$ -th hierarchical component  $X_{k,e}$  for the  $k$ -th layer can be obtained using equation (6) based on the operator matrix  $Q_j^k$ .

$$X_{k,e} = Q_{r_k}^k \bullet Q_{r_{k-1}}^{k-1} \bullet \dots \bullet Q_{r_1}^1 \bullet X \quad (6)$$

where  $e$  is hierarchical node number. For a nonnegative integer  $e$ , there is a unique vector  $[r_1, r_2, \dots, r_k]$  corresponding to it based on equation (7).

$$e = \sum_{\lambda=1}^k 2^{k-\lambda} r_\lambda \quad (7)$$

where  $\{r_\lambda, \lambda=1, \dots, k\} \in \{0, 1\}$ .

**Step 4** Repeat Steps (1)–(3) for each node until all  $(2^{n+1}-1)$  hierarchical components are obtained.

**Step 5** Calculate the SSE value of hierarchical components for each layer and then augment the SSE value as follows.

$$\text{EHSSE}_{1:j} = \{\text{EHSSE}_{1:j-1}; \text{SSE}(X_{k,e}, m, \varepsilon)\} \quad (8)$$

In the enhanced hierarchical decomposition procedure, since both the modified averaging and differential procedures are utilized, EHSSE can extract fault features from both low- and high-frequency component. For better understanding, the enhanced hierarchical analysis is illustrated in the hierarchical tree diagram, Figure 1. In summary, pseudocode of EHSSE is shown in Algorithm 1 and the flowchart of EHSSE is illustrated in Figure 2.

### Algorithm 1: EHSSE

---

**Input:**  $X$ : Time domain signal  
 $m$ : Embedding dimension  
 $\varepsilon$ : Symbol number  
 $n$ : Number of hierarchical layer  
**Output:** EHSSE: the entropy value

**1 for**  $k \in [1, n]$  **do**

**2 Conduct the operator matrix**  $Q_j^k$   
     **Generate the hierarchical component**  $X_{k,e}$   
     **Calculate the SSE value of**  $X_{k,e}$   
     **Augment the value**  
      $\text{EHSSE}_{1:k} = \{\text{EHSSE}_{1:k-1}; \text{SSE}(X_{k,e}, m, \varepsilon)\}$

**3 endfor**

---

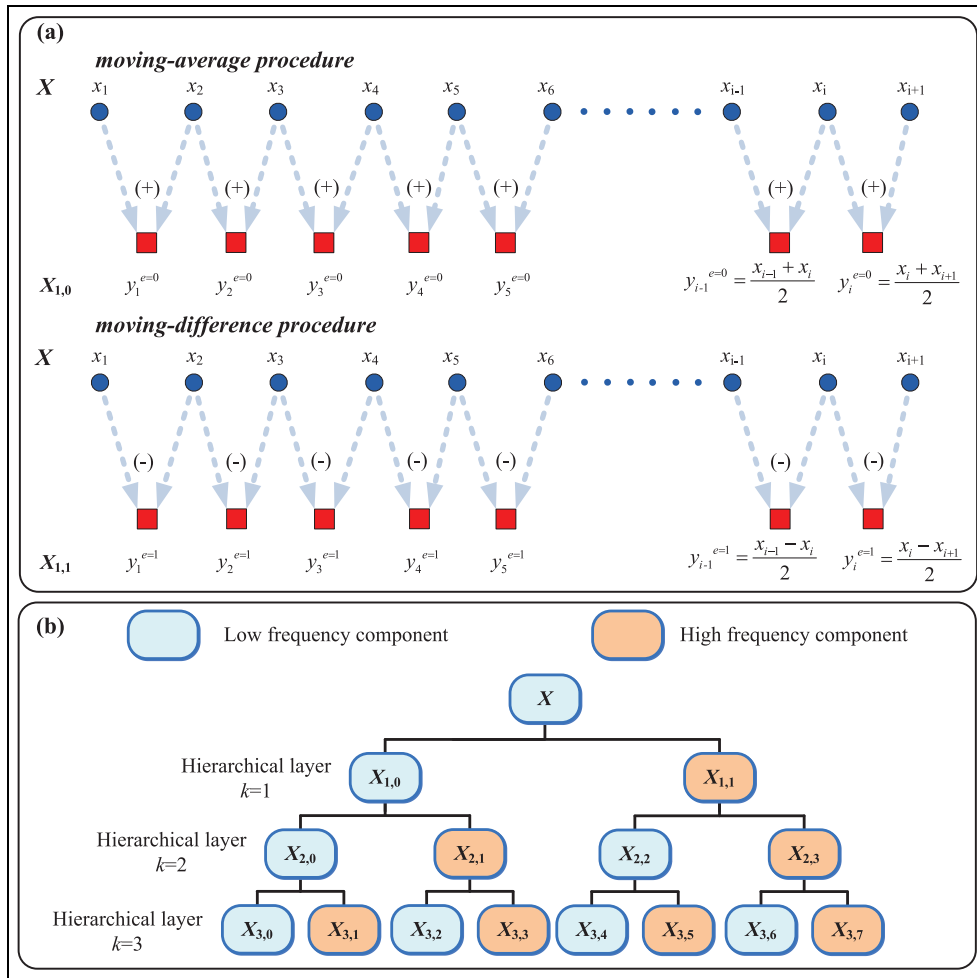


**Figure 1.** Schematic diagram of the enhanced hierarchical analysis: (a) modified moving-average and moving-difference procedure and (b) hierarchical tree.

In the article, enhanced hierarchical analysis is proposed using modified moving-averaging and moving-difference process to extract information from both low- and high-frequency components. To demonstrate this property, the simulated gear signal in “Impulse detection” is used. Here, the signal of slight fault condition is analyzed using enhanced hierarchical analysis, and the spectrum of two hierarchical signals under layer  $n=2$  is obtained as shown in Figure 3. It can be found from Figure 3 that there are more low-frequency components in hierarchical signal  $X_{2,0}$ , and there are more high-frequency components in hierarchical signal  $X_{2,3}$ . The phenomenon indicates that the proposed hierarchical analysis can extract information from both low- and high-frequency components.

## Simulation evaluation

In this section, the simulated signals have been implemented to verify the superiority of SSE by comparing

with SE, FE, and PE methods. Here, the parameter setting of SSE is as follow:  $m=2$ ,  $\varepsilon=5$ . In addition, the corresponding parameters of SE, FE, and PE are selected following Li et al.<sup>11</sup> and Zhang et al.<sup>29</sup> The embedding dimension  $m$  of PE are set as:  $m=6$  following Zhang et al.<sup>29</sup> The two parameters of SE and FE are set as:  $m=2$  and the tolerance  $r=0.15$  following Li et al.<sup>11</sup> The effectiveness of the parameters of SE, FE, and PE methods has been verified using both simulated and experimental signals in the mentioned references.

## Robustness

In order to study the noise robustness of SSE, four types of basic signals: frequency modulate signal, amplitude modulate signal, frequency and amplitude modulate signal, and sinusoid signal are studied. The four signals can be expressed in equations (9) to (12).

$$y = \sin(2\pi \times 0.1 \times 1.0312^t t) \quad (9)$$

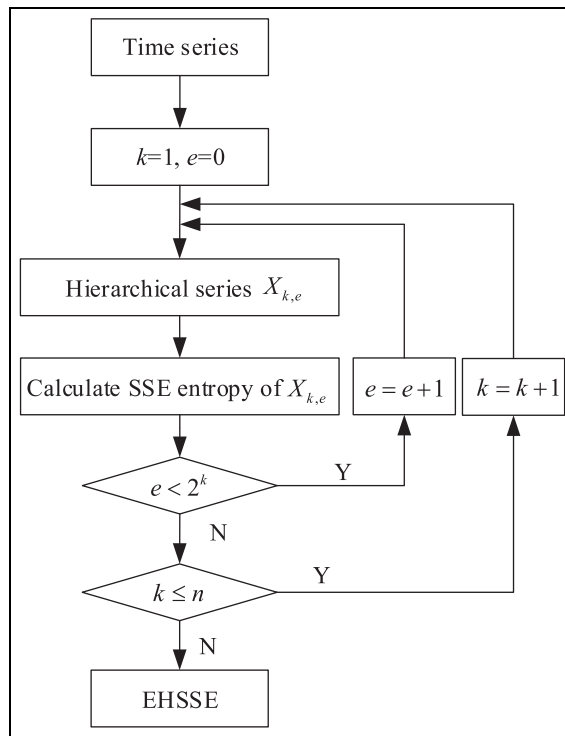


**Figure 2.** Flowchart of enhanced hierarchical symbolic sample entropy

$$y = \sin(2\pi t) \times \sin(0.2\pi t) \quad (10)$$

$$y = \sin(2\pi \times 0.1 \times 1.0312^t \times t) \times \sin(0.2\pi t) \quad (11)$$

$$y = \sin(2\pi t) \quad (12)$$

We add white Gaussian noise at different noise levels into four types of basic signals to study the robustness. It is noticed that SNR value varies from 30 to 0 dB and the step is 1 dB. Here, each signal contains 2048 points and the sampling frequency is 16 Hz. The obtained simulated signals are illustrated in Figure 4. Because the values of these four methods are not in the

same dimension and a direct comparison between the entropy values will fail to accurately show the robustness. Therefore, the rate of increment for each method is calculated for comparing the robustness. The rate of increment  $I$  is defined as equation (13).

$$I = \frac{H - H_0}{H_0} \times 100\% \quad (13)$$

where  $H$  represents entropy value under current SNR environment and  $H_0$  represents entropy value of initial SNR environment. Here,  $H_0$  is the entropy value of SNR = 30 dB.

To reduce randomness, 10 trials are performed. The average increment rate  $I$  of four entropy methods is given in Figure 5. Obviously, the higher the increment rate, the worse the robustness for the same SNR is. As seen from Figure 5, SSE obtains the slowest increasing rate in the four basic signal tests. To get an intuitive result, the threshold is set as 10%. From Figure 5, we can obtain the point where the increasing rate exceeds the threshold, shown in Table 1.

From Table 1, it can be observed that SSE curve has the smallest critical point value and the critical point is 5, 16, 8, and 6 dB for four signals, respectively. The phenomenon indicates that SSE performs best in robustness than other methods in comparison. In addition, as seen from Figure 3, it can be found that SSE has the smallest standard deviation in the four basic signal tests. In summary, SSE has the best robustness ability with smallest increasing rate and standard deviation in four basic signal tests, which means that SSE can work with heavier background noise than SE, FE, and PE.

### Impulse detection

To verify the performance of SSE in fault-related transient identification, signals corresponding to gear fault

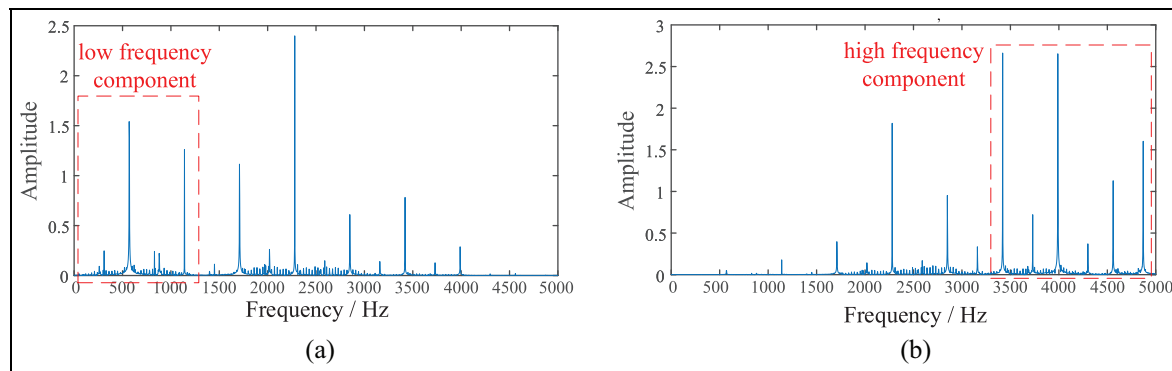


**Figure 3.** The examples of information extraction from high- and low-frequency components for enhanced hierarchical analysis: the spectrum of (a)  $X_{2,0}$  and (b)  $X_{2,3}$ .

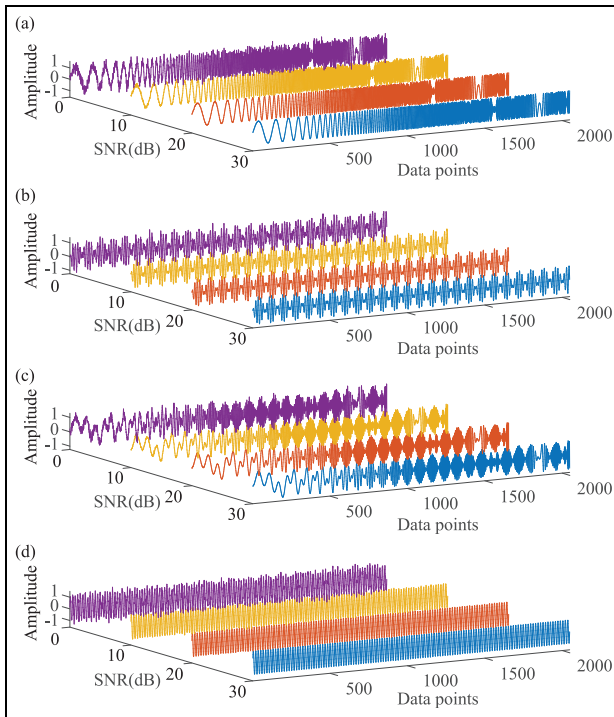


**Figure 4.** Four basic signals: frequency modulate signal (FM), amplitude modulate signal (AM), frequency and amplitude modulate signal (FM-AM), and sinusoid signal (SIN) with different SNR: (a) FM, (b) AM, (c) FM-AM, and (d) SIN.

**Table I.** The critical points of four entropy methods in noise testing.

Method	SSE (dB)	PE (dB)	FE (dB)	SE (dB)
FM	5	24	24	25
AM	16	25	24	27
FM-AM	8	23	23	25
SIN	6	22	24	25

AM: amplitude modulate signal; FE: fuzzy entropy; FM: frequency modulate signal; FM-AM: frequency and amplitude modulate signal; SSE: symbolic sample entropy; SIN: sinusoid signal; SE: sample entropy; PE: permutation entropy.

are simulated as per Liang et al.<sup>30</sup> Table 2 lists the parameters of a spur gearbox. A dynamic model is used and three types of pitting levels are simulated, including slight pitting, medium pitting, and severe pitting. Note that the signals of three types of levels are spliced into one signal and the data length of generated signal is 61,440, as illustrated in Figure 6(a). Here, sliding windows of length 2048 data points at a step length of 512 is used for cutting out the signal. In order to assess the fault-related transient identification ability, the first five samples are considered as the normal sample and absolute distance of other samples from the first five samples are calculated, as shown in Figure 6(b) to (e).

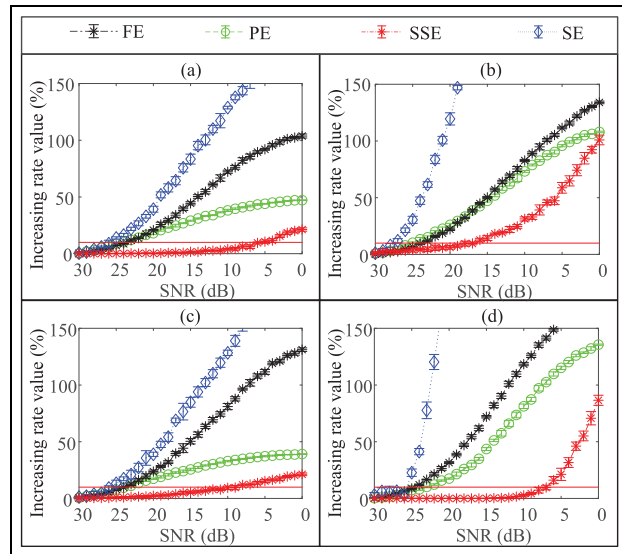


**Figure 5.** The performances of four entropy statistics on robustness for four basic signals: (a) frequency modulate signal (FM), (b) amplitude modulate signal (AM), (c) frequency and amplitude modulate signal (FM-AM), and (d) sinusoid signal (SIN).

From Figure 6(b) and (d) it can be seen that SE and PE can hardly detect the impulses and represent large fluctuation when periodical impulses are generated. This phenomenon indicates that SE and PE have poor ability to distinguish the noise and periodical impulses. On the contrary, FE has less fluctuation than SE since FE has utilized fuzzy set theory for complexity measure so that FE obtains more robust results in impulse detection. However, FE can hardly detect the impulses derived from slight fault. In comparison to other methods, our proposed SSE can track all periodical impulses derived from three crack fault severities with least fluctuation, as illustrated in Figure 6(e). In summary, it is validated that the SSE algorithm has the best ability in impulse detection.

### Calculational efficiency

The computational complexity for SE, FE, and PE are  $O(n^2)$ ,  $O(n^2)$ , and  $O(n)$ , respectively,<sup>31,32</sup> as shown in Table 3. According to the definition of SSE, SSE has a computational complexity of  $O(n)$ . In addition, in order to intuitively investigate the calculational efficiency, the calculation time of simulated signals in “Impulse detection” is counted and the results for four entropy method are presented in Table 3. It is noticed that a core i5-9400F@2.9GHz computer with 16 GB RAM is used. The matlab version utilized is R2018. As for the simulated signals, computational cost of SSE is 20 times lower in compare to other entropy methods. The phenomenon indicates that the combination of SE

**Table 2.** Parameter setting of the simulated gear set.

Parameters	Pinion (driving)	Gear (driven)
Number of teeth	19	31
Number of teeth	3.2	3.2
Pressure angle	20°	20°
Mass (kg)	0.700	1.822
Face width (m)	0.0381	0.0381
Young's modulus (Pa)	$2.068 \times 10^{11}$	$2.068 \times 10^{11}$
Poisson's ratio	0.3	0.3
Base circle radius (mm)	28.3	46.2
Root circle radius (mm)	26.2	45.2
Bearing stiffness (N/m)	$k_1 = k_2 = 5.0 \times 10^8$	
Bearing damping (kg/s)	$c_1 = c_2 = 4.0 \times 10^5$	
Torsional stiffness of shaft coupling (N/m)	$k_p = k_g = 4.0 \times 10^7$	
Torsional damping of shaft coupling (kg/s)	$c_p = c_g = 3.0 \times 10^4$	

**Table 3.** Computational complexity and calculation time of SE, FE, PE, and SSE entropy methods.

Method	Computational complexity	Calculation time (s)
SE	$O(n^2)$	34.48
PE	$O(n)$	25.18
FE	$O(n^2)$	153.24
SSE	$O(n)$	1.25

SE: sample entropy; PE: permutation entropy; FE: fuzzy entropy; SSE: symbolic sample entropy.

and SDF can improve significantly the calculation efficiency.

### Parameter Analysis

Values of three parameter  $m$ ,  $k$ , and  $\varepsilon$  are needed to be determined for the proposed method. The dimension  $m$  denotes the length of vectors to be matched. Here, relevant dynamic process can be reconstructed in more detailed manner with a larger  $m$  value. On the contrary, a large value of  $m$  results in a longer time-series, which is difficult to achieve in practical application. According to Chen et al.,<sup>16</sup> value of  $m$  is taken as 2. The number of hierarchical layers  $k$  is related to the numbers of features. A small number of hierarchical layer will result in poor performance of feature extraction, and a large layer will lead to dimensionality disaster and increasing calculation cost. Hence, here,  $n$  is recommended to be set as 3 in this study.

As the last parameters, symbol number is represented by  $\varepsilon$ . Logistic dataset  $\{x|x_{i+1}=Rx_i(1-x_i)\}$  has been used to study the performance of SSE for different values of  $\varepsilon$  (where  $x_1$  is set as 0.1). Values of  $\varepsilon$  are selected for different values of  $R$  such as  $R=3.5$ ,  $3.7$ ,

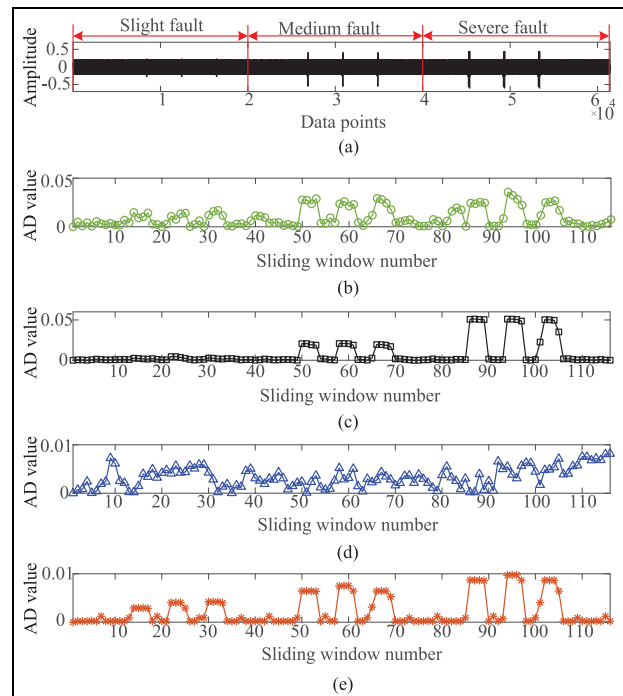


**Figure 6.** Comparison of impulse detection ability of different entropy methods: (a) time-series of simulated gearbox fault signal, (b) SE, (c) FE, (d) PE, and (e) SSE.  
SE: sample entropy; PE: permutation entropy; FE: fuzzy entropy; SSE: symbolic sample entropy.

3.8, and 3.9. The sequence is generated following 200 points, and length  $N$  of time-series is 1000. It is worth noting that  $R=3.5$  produces periodic dynamic behavior, while  $R=3.7$ –3.9 produces signals with increasing complexity. Due to the fact that the higher the complexity, the higher the entropy, theoretically, the entropy value order of four signals should be listed as:  $En_{R=3.5} < En_{R=3.7} < En_{R=3.8} < En_{R=3.9}$ . The obtained entropy values with different  $\varepsilon$  are illustrated in Figure 7. As can be seen, a mixing phenomena happens for the value of  $\varepsilon$  as 3. However, for  $\varepsilon$  values more than 5, SSE values are well in coordination with the values of  $R$ . Generally, with the incorporation of more and more symbols, noise resistance ability gradually decreases. On the contrary, the smaller the number of symbols, the more serious the information loss, thus making it difficult for SSE to extract sufficient and useful fault information. Hence,  $\varepsilon$  is advised to be set as 5–15, and  $\varepsilon=10$  is selected in the further experimental study.

### Flowchart of proposed intelligent fault diagnosis method

In this study, a rotating machinery fault diagnosis approach is proposed based on EHSSE algorithm. The

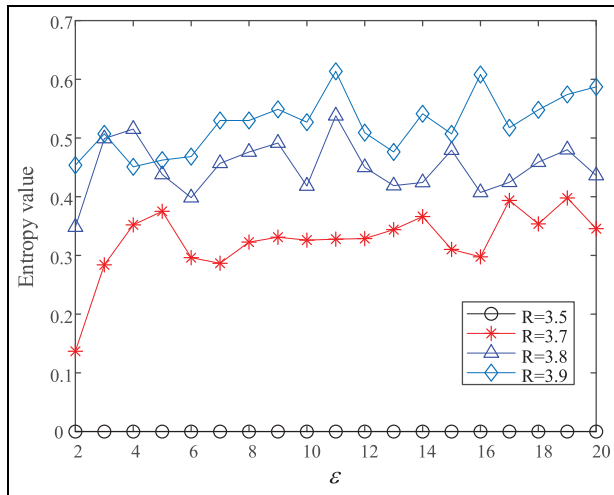


**Figure 7.** Performance of SSE with different parameter  $\epsilon$ .

overall framework is illustrated in Figure 8 and the detailed procedures can be summarized as follows:

- (1) The data acquisition under different health conditions is conducted.
- (2) The data is segmented into signal samples for each condition and samples are divided into the training set and testing set.
- (3) EHSSE is employed to quantify nonlinearity and characterize fault information from the vibration signals.
- (4) The obtained entropy features of the training set are fed into support vector machine (SVM) to train a classifier.
- (5) Test the trained SVM classifier using features of testing set and accomplish the fault pattern recognition of rotating machinery.

It is pertinent to mention here that we utilize a grid search approach<sup>33</sup> with fivefold cross-validation<sup>34</sup> to conduct the optimization of SVM.

## Case studies

In this Section, two experimental case studies are carried out to assess the superiority of EHSSE-based algorithm for fault diagnosis of rotating machinery.

### Case study I

**Test rig.** The first case study was conducted on a planetary gearbox system, as shown in Figure 9. The test rig is mainly composed of the driving motor, tachometer, planetary gearbox and magnetic damping. Specifications of planetary gearbox are listed in Table

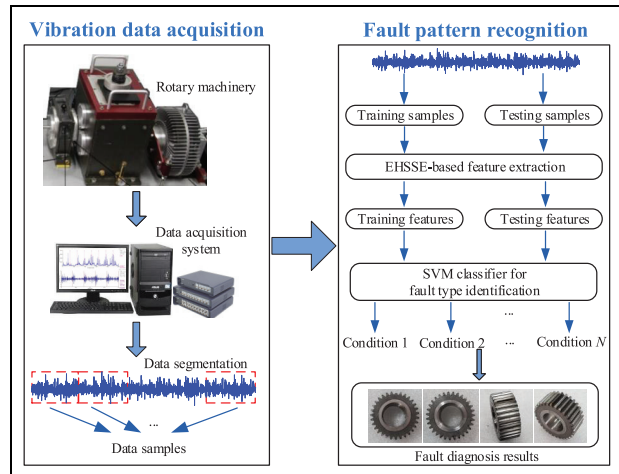


**Figure 8.** The flowchart of EHSSE-based diagnosis approach.

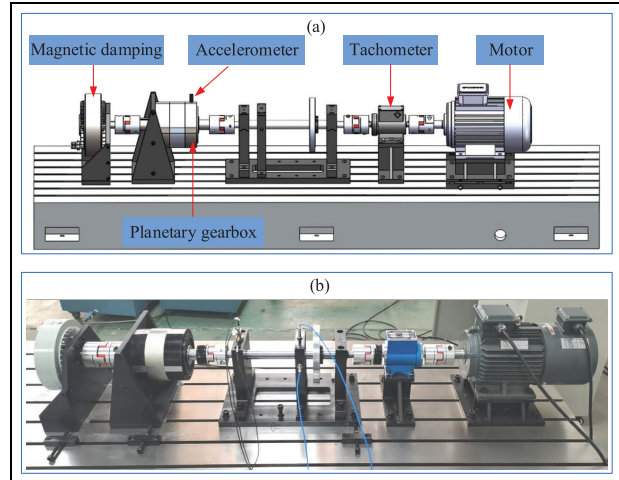


**Figure 9.** The planetary gearbox system of case study I: (a) the layout of the test rig and (b) the experimental test rig. PGBT: planet gear with a broken tooth; PGCT: planet gear with a cracked tooth; PGST: planet gear with a spalling tooth; PGWT: planet gear with a wearing tooth.

4. An accelerometer was installed on the top of planetary gearbox casing to collect the vibration signals. In the case study, the different types of damages include wearing tooth, broken tooth, cracked tooth, and spalling tooth, as illustrated in Figure 10. In this case study, data sampling frequency is 16 kHz and the rotation speed is set as 1200 rpm. Moreover, the 5 Nm load is designed to simulate real-world applications.

In total five types of health conditions are considered in this experimental case study, including healthy gear, planet gear with a broken tooth (PGBT), planet gear with a spalling tooth (PGST), planet gear with a cracked tooth (PGCT), and planet gear with a wearing

**Table 4.** Configuration parameters of the planetary gearbox for case study I.

Parameter	Value
Rotating speed	1200 rpm
Load	5 Nm
Sample frequency	16 kHz
Number of teeth for sun gear	21
Number of teeth for planet gear	31
Number of teeth for ring gear	84

**Table 5.** Description of the analyzed planetary gearbox system fault patterns for case study I.

Fault class	Class label	Number of training data	Number of testing data
Normal	1	75	25
PGBT	2	75	25
PGST	3	75	25
PGCT	4	75	25
PGWT	5	75	25

PGBT: planet gear with a broken tooth; PGST: planet gear with a spalling tooth; PGCT: planet gear with a cracked tooth; PGWT: planet gear with a wearing tooth.

**Table 6.** Diagnosis results of planetary gearbox system for case study I.

Method	Mean testing accuracy (%)	Standard deviation (%)
EHSSE	99.88	0.17
MSSE	89.28	2.76
EHSSE	98.72	0.89
MSE	33.84	23.99
MFE	91.48	2.14
MPE	90.28	2.99

EHSSE: enhanced hierarchical symbolic sample entropy;  
MSSE: multiscale symbolic sample entropy.

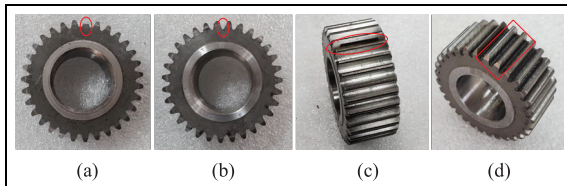


**Figure 10.** Figure 10. (a) PGBT, (b) PGCT, (c) PGST, and (d) PGWT.

PGBT: planet gear with a broken tooth; PGCT: planet gear with a cracked tooth; PGST: planet gear with a spalling tooth; PGWT: planet gear with a wearing tooth.

tooth (PGWT), as shown in Table 5. It is noticed that there are 100 samples for each health condition and this case study contains total 500 samples as shown in

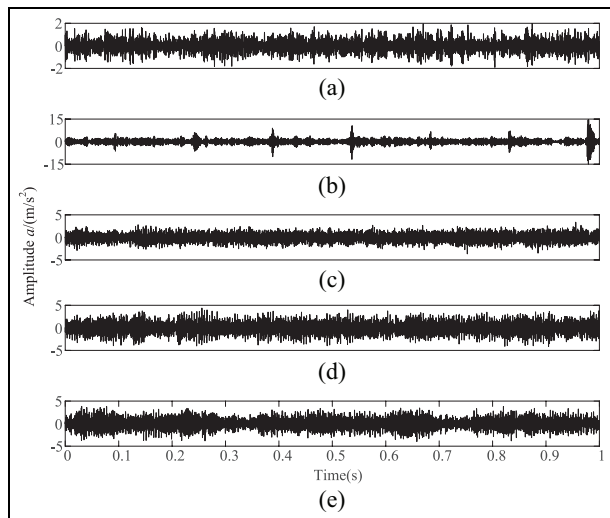


**Figure 11.** The time-domain waveforms of five health conditions for planetary gearbox: (a) healthy gear, (b) PGBT, (c) PGST, (d) PGCT, and (e) PGWT.

PGBT: planet gear with a broken tooth; PGCT: planet gear with a cracked tooth; PGST: planet gear with a spalling tooth; PGWT: planet gear with a wearing tooth.

Table 5. The measured vibration signals under different types of fault states as well as health working condition are shown in Figure 11.

**Experimental results.** To verify the feature performance of the proposed method, existing entropy methods, including MSE, MPE, and multiscale fuzzy entropy (MFE) are also utilized to extract the weak fault characteristics. In addition, multiscale symbolic sample entropy (MSSE) and enhanced hierarchical sample entropy (EHSSE) are also implemented to verify the advantage of symbolization and enhanced hierarchical analysis, respectively. Here, we set scale parameter  $\tau = 15$  in multiscale-based entropy methods for MSE, MFE, MPE, and MSSE methods. Also, we set the hierarchical parameter  $k = 3$  in EHSE and proposed EHSSE. The other parameter settings of comparison methods are as follows:  $m = 2$  and  $r = 0.15$  in MSE and EHSE;  $m = 6$  in MPE;  $m = 2$  and  $r = 0.15$  in MFE;  $m = 2$  and  $\varepsilon = 10$  in MSSE. Note that 20 trials are conducted to reduce the randomness effect on the final results. The obtained diagnostic results of six methods are given in Table 6.

It can be observed from Table 6 that among six methods, EHSSE method obtains the highest classification accuracy of 99.88% with the smallest standard deviation of 0.17%. The accuracy order is: EHSSE > EHSE > MFE > MPE > MSSE > MSE, which further confirms the superiority of EHSSE in feature extraction. First, it implies that the feature extraction

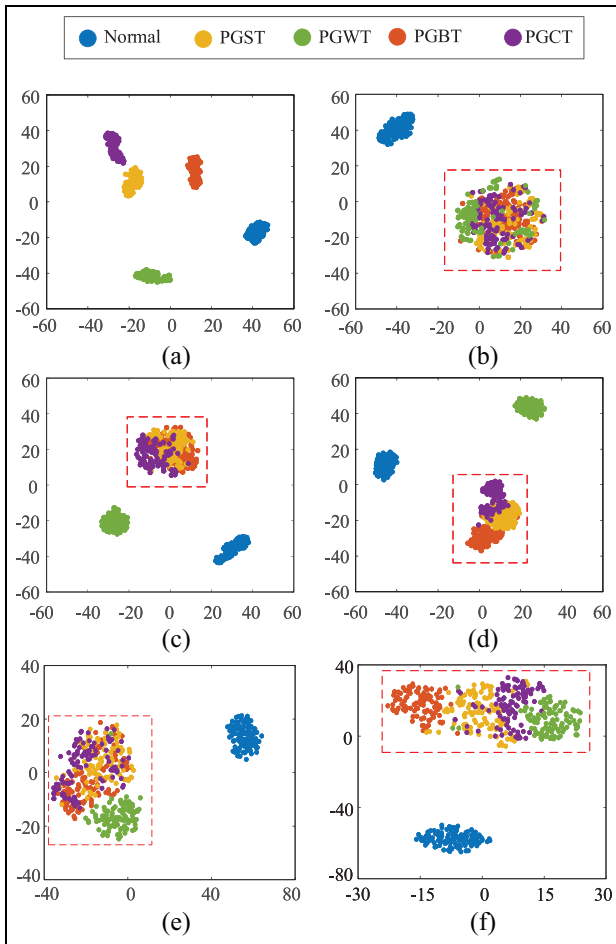


**Figure 12.** Feature visualization of case study I via t-SNE: feature representations extracted by four entropy methods: (a) EHSSE, (b) MSE, (c) MFE, (d) MPE, (e) MSSE, and (f) EHSE. EHSSE: enhanced hierarchical symbolic sample entropy; MSSE: multiscale symbolic sample entropy; EHSE: enhanced hierarchical sample entropy.

ability of EHSSE has been greatly improved than the original MSE method. Second, compared with EHSE, MSSE, and MSE methods, it can be found that the feature extraction capability of SE can be also enhanced via combination with SDF or enhanced hierarchical analysis. This is because that EHSSE method deeply incorporates the advantages of SDF and enhanced hierarchical analysis. The symbolization processes can reduce the noises so that our EHSSE method has better performance in denoising ability. Moreover, the enhanced hierarchical analysis is proposed to extract more fault information with higher stability compared with the traditional multiscale-based entropy methods.

For further analysis, the visualization representation of all entropy feature distributions is given in Figure 12. In order to intuitively analyze the feature space, we applied the *t*-distributed stochastic neighbor

embedding (*t*-SNE) algorithm to project the features onto a two-dimensional space. The cluster ability indicates the feature extraction ability: the smaller inner-class distance among samples within the same cluster and the larger inter-class distance among clusters, the better the feature extraction ability of the entropy method. As can be seen from Figure 12(a), EHSSE features of the five different types have been clustered and each cluster can be clearly separated. However, the feature representation of other entropy methods is mixed. Therefore, there is a nice clustering result for EHSSE when comparing with the other entropy-based methods, which further verify the superiority of EHSSE in extracting the fault information.

It also can be seen that MSSE method performs better compared with MSE method due to that the condition of PGWT can be separated using MSSE method. The phenomenon validates the advantage of SDF. Moreover, from Figure 12(b) and (f), it can be found that the four conditions of PGWT, PGBT, PGCT, and PGST have clearer boundary compared with MSE method. Overall, both enhanced hierarchical analysis and SDF are effective to enhance the feature extraction ability.

## Case study II

**Test rig.** In this experiment, rubbing fault of a rotor test rig and faults of bearing operating under different working condition have been studied. Experimental set up is demonstrated in Figure 13, which mainly consists of rotating shaft, blade disc, casings, bearings, and sensor. Here, data sampling frequency is 10 kHz and the rotation speed is constant with 3000 rpm.

During the experimental process, ten working conditions are carried out, including normal condition, six single-fault conditions and three compound fault conditions. The six single-fault conditions include full annular rubbing (FAR), cracked blade, crack in bearing inner ring (CIR), crack in bearing outer ring, cracked leaf disc (CLD), shaft rubbing (SR). Here, rotor FAR denotes that the rotor is always in contact with a fixed point and SR represents that the shaft contacts with a fixed point of stator. Meanwhile, the three compound fault conditions include shaft rubbing with crack in bearing inner ring (SR-CIR), crack of leaf disc with shaft rubbing (CLD-SR), and full annular rubbing with shaft rubbing (FAR-SR).

It is noticed that there are 100 samples for each health condition and this case study contains total 1000 samples. These details are given in Table 7. Figure 14 illustrates signals under 10 working conditions. Then, the diagnostic process shown in Figure 8 is utilized for fault pattern recognition. Also, the accuracy of 20 tests

**Table 7.** Description of the analyzed rotor system fault patterns for case study II.

Fault class	Class label	Number of training data	Number of testing data
Normal	1	75	25
FAR	2	75	25
CB	3	75	25
CIR	4	75	25
COR	5	75	25
CLD	6	75	25
SR	7	75	25
SR-CIR	8	75	25
SR-CLD	9	75	25
FAR-SR	10	75	25

CB: cracked blade; CIR: crack in bearing inner ring; COR: crack in bearing outer ring; CLD: crack of leaf disc; SR: shaft rubbing; SR-CIR: shaft rubbing with cracked inner race; SR-CLD: shaft rubbing with crack of leaf disc; FAR: full annular rubbing; FAR-SR: full annular rubbing with shaft rubbing.

**Table 8.** Diagnosis results of rotor system for case study II.

Method	Mean testing accuracy (%)	Standard deviation (%)
EHSSE	99.58	0.39
MSSE	87.38	1.49
EHSE	95.24	1.16
MSE	63.74	2.91
MFE	96.56	1.14
MPE	85.90	1.46

EHSSE: enhanced hierarchical symbolic sample entropy; MSSE: multiscale symbolic sample entropy; EHSE: enhanced hierarchical sample entropy.

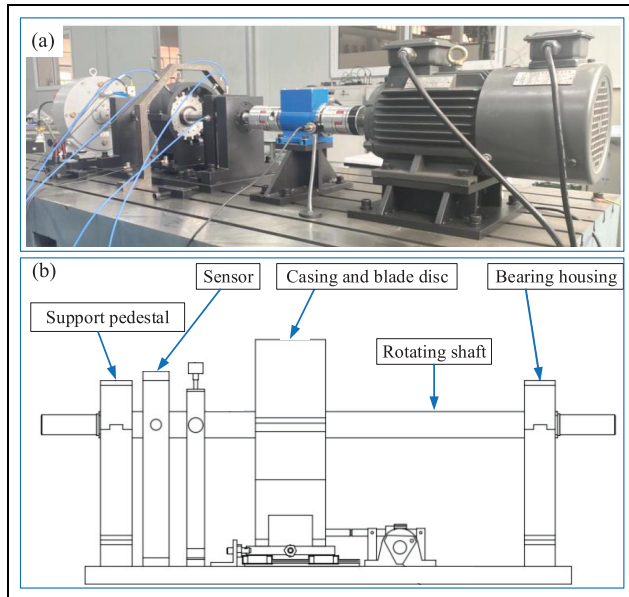


**Figure 13.** The sketch of the rotor test rig: (a) rotor test rig and (b) component diagram of rotor test rig.

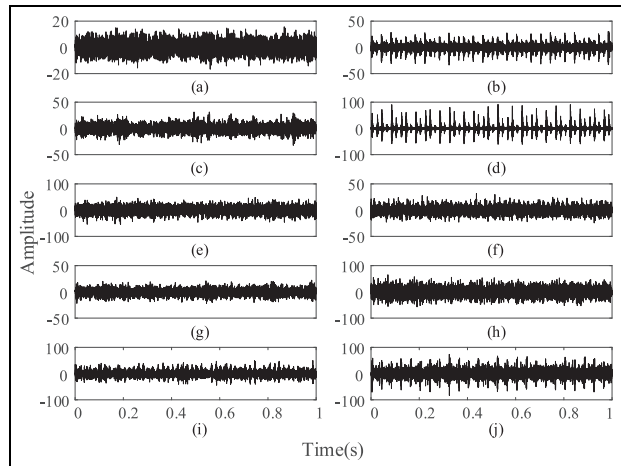


**Figure 14.** The time-domain signals of 10 working conditions for rotor system: (a) healthy condition, (b) full annular rubbing, (c) cracked blade, (d) crack in bearing inner ring, (e) crack in bearing outer ring, (f) cracked leaf disc, (g) shaft rubbing, (h) shaft rubbing with cracked inner race, (i) crack of leaf disc with shaft rubbing, and (j) full annular rubbing with shaft rubbing.

is used to verify the superiority of proposed EHSSE-based method.

**Experimental results.** Like case study I, EHSSE is firstly applied to extract features with hierarchical layer  $n=3$ . Next, SVM is employed for pattern recognition. In addition, MSSE, EHSE, MSE, MFE, and MPE are all employed for comparison and the diagnostic results are presented in Table 8.

Generally, the diagnostic performance for each method is similar to case study I. In this context, the experimental results can be summarized as follows. First, the highest mean classification accuracy can be obtained by the proposed EHSSE with 99.58%, which further validates the superiority of EHSSE in fault characteristic extraction. Meanwhile, the accuracy order is: EHSSE > MFE > EHSE > MSSE > MPE > MSE. Second, EHSSE obtains the smallest standard deviation value of 0.39%, which confirms the stability advantage of enhanced hierarchical analysis. Finally, as the improved methods of MSE, MSSE, and EHSE perform better than the original MSE method, which verify the effectiveness of SDF and enhanced hierarchical analysis respectively.

Also, two-dimensional figures can be obtained using t-SNE approach, as shown in Figure 15. It is found from Figure 15(a) that there are 10 distinct class centers which makes the classification task easy for SVM. On the contrary, for other entropy algorithms, some of the samples are scattered away from the distinct class.

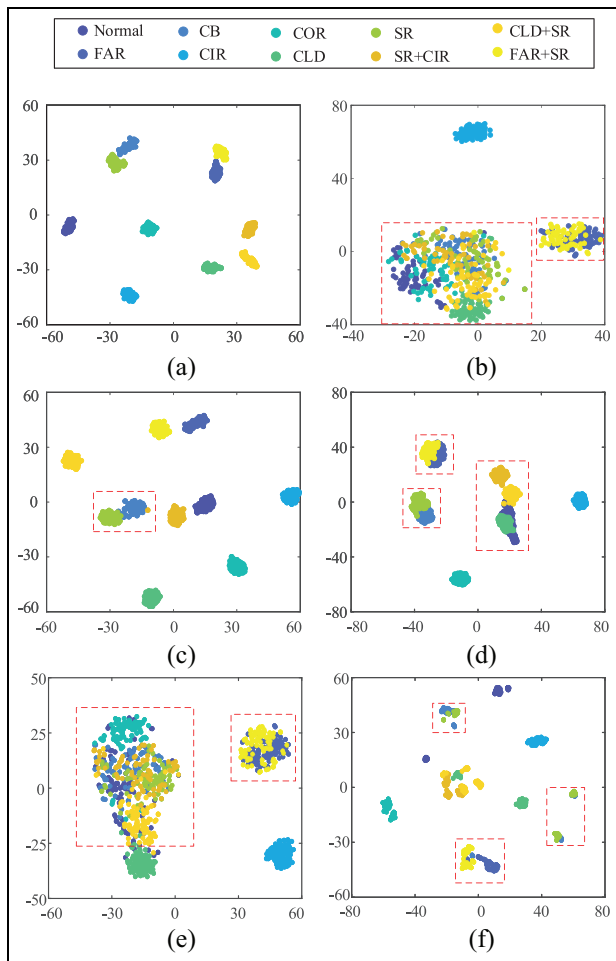


**Figure 15.** Feature visualization of case study II via t-SNE: feature representations extracted by four entropy algorithms: (a) EHSSE, (b) MSE, (c) MFE, (d) MPE, (e) MSSE, and (f) EHSE. EHSSE: enhanced hierarchical symbolic sample entropy; MSSE: multiscale symbolic sample entropy; EHSE: enhanced hierarchical sample entropy.

This validates the effectiveness of EHSSE in feature extraction. Among them, MSE performs worst due to the high degree of scattering of relevant samples and indistinguishable boundary condition. Compared with MSE method, the features generated using MSSE and EHSE has a better clustering phenomenon as shown in Figure 15(b), (e), and (f). This is because the combination of SDF can reduce the noise-related fluctuations and increase the robustness under low-SNR environment. Moreover, the combination of enhanced hierarchical analysis can capture comprehensively the fault characteristics from both high-frequency and low-frequency components. Hence, MSSE and EHSE has a better feature extraction ability compared with original MSE method.

Efficiency of the proposed method is assessed by varying the percentages of training samples (the rest

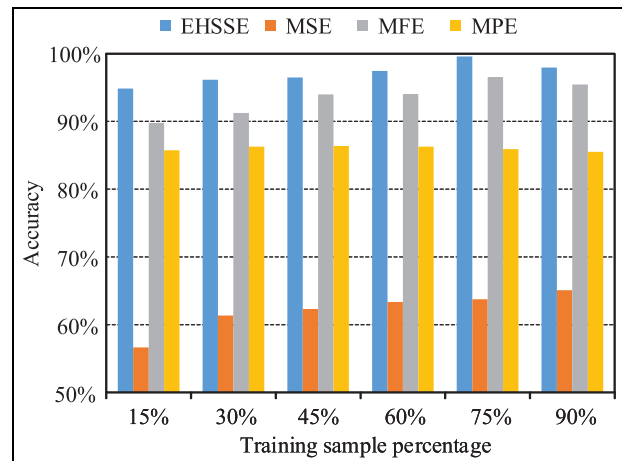


**Figure 16.** Performance of EHSSE, MSE, MFE, and MPE methods under different number of training samples.  
EHSSE: enhanced hierarchical symbolic sample entropy.

samples are used as test samples) as 15%, 30%, 45%, 60%, 75%, and 90%. For ensuring the robustness, 20 trials are performed for each selected percentages of test data. Figure 16 illustrates the mean testing accuracies. As seen from Figure 16, the testing accuracy show a general upward trend as the training samples increase. Among four entropy-based methods, EHSSE achieves the best performance by obtaining the highest accuracy for varying percentages of training data.

## Conclusions

In the study, a novel complexity measure indicator termed as EHSSE is proposed by incorporating SSE and enhanced hierarchical analysis. The SSE is robust to noise interference via introducing the SDF process. Meanwhile, enhanced hierarchical analysis can extend SSE to extract the fault information of both low and high components from vibration signals. Two case studies are conducted to demonstrate its advantage in classifying various faults of rotating machinery. Results show that the proposed strategy achieves the highest recognition ratios with 99.88% and 99.58%, respectively, which is much higher than the state-of-the-art entropy technologies, including MSE, MPE, and MFE. The main contributions of this article are summarized as follows:

- (1) SSE has merits of stability and strong robustness to interference by introducing the SDF process.
- (2) By incorporating SSE and enhanced hierarchical analysis, EHSSE is proposed, which can extend SSE to extract the fault information of both low and high components from vibration signals.

- (3) Two experiments are designed and results indicate the EHSSE-based fault diagnosis method has superior performance and obtains the excellent recognition ratios than other entropy methods.

In this preliminary study, the combination of SDF process, SE method and enhanced hierarchical analysis algorithm, namely EHSSE has been verified to be a promising solution for achieving pattern recognition and fault diagnosis. In the future, efforts will be put to assess the efficiency of EHSSE with variable working conditions in a more realistic environment.

### Declaration of conflicting interests

The author(s) declared no potential conflicts of interest with respect to the research, authorship, and/or publication of this article.

### Funding

The author(s) disclosed receipt of the following financial support for the research, authorship, and/or publication of this article: The research was supported in part by National Natural Science Foundation of China, China [Grant No. 51805434 and 12172290], Key Laboratory of Equipment Research Foundation, China [Grant No. 6142003190208].

### ORCID iD

Yongbo Li  <https://orcid.org/0000-0003-2699-9951>

### References

1. Du Y, Zhou S, Jing X, et al. Damage detection techniques for wind turbine blades: A review. *Mech Syst Signal Process* 2020; 141: 106445.
2. Li Y, Zuo MJ, Chen Z, et al. Railway bearing and cardan shaft fault diagnosis via an improved morphological filter. *Struct Health Monit* 2020; 19(5): 1471–1486.
3. Wang Z, Yang N, Li N, et al. A new fault diagnosis method based on adaptive spectrum mode extraction. *Struct Health Monit* 2021; 20(6): 3354–3370.
4. Wang T, Lu G, Liu J, et al. Graph-based change detection for condition monitoring of rotating machines: techniques for graph similarity. *IEEE Trans Reliab* 2018; 68(3): 1034–1049.
5. Elasha F, Greaves M and MBA D. Planetary bearing defect detection in a commercial helicopter main gearbox with vibration and acoustic emission. *Struct Health Monit* 2018; 17(5): 1192–1212.
6. Wan S and Zhang X. Bearing fault diagnosis based on teager energy entropy and mean-shift fuzzy c-means. *Struct Health Monit* 2020; 19(6): 1976–1988.
7. Liang X, Zuo MJ and Hoseini MR. Vibration signal modeling of a planetary gear set for tooth crack detection. *Eng Fail Anal* 2015; 48: 185–200.
8. Feng Z and Zuo MJ. Vibration signal models for fault diagnosis of planetary gearboxes. *J Sound Vibr* 2012; 331(22): 4919–4939.
9. Zhang M, Wang K, Wei D, et al. Amplitudes of characteristic frequencies for fault diagnosis of planetary gearbox. *J Sound Vibr* 2018; 432: 119–132.
10. Feng Z, Lin X and Zuo MJ. Joint amplitude and frequency demodulation analysis based on intrinsic time-scale decomposition for planetary gearbox fault diagnosis. *Mech Syst Signal Process* 2016; 72: 223–240.
11. Li Y, Wang X, Si S, et al. Entropy based fault classification using the case western reserve university data: a benchmark study. *IEEE Trans Reliab* 2019; 69(2): 754–767.
12. Udhayakumar RK, Karmakar C and Palaniswami M. Approximate entropy profile: a novel approach to comprehend irregularity of short-term HRV signal. *Nonlinear Dyn* 2017; 88(2): 823–837.
13. Bandt C and Pompe B. Permutation entropy: a natural complexity measure for time series. *Phys Rev Lett* 2002; 88(17): 174102.
14. Li Y, Yang Y, Li G, et al. A fault diagnosis scheme for planetary gearboxes using modified multi-scale symbolic dynamic entropy and mRMR feature selection. *Mech Syst Signal Process* 2017; 91: 295–312.
15. Zheng J and Pan H. Use of generalized refined composite multiscale fractional dispersion entropy to diagnose the faults of rolling bearing. *Nonlinear Dyn* 2020; 101(2): 1417–1440.
16. Chen W, Zhuang J, Yu W, et al. Measuring complexity using fuzzyen, apen, and sampen. *Med Eng Phys* 2009; 31(1): 61–68.
17. Landauskas M, Cao M and Ragulskis M. Permutation entropy-based 2d feature extraction for bearing fault diagnosis. *Nonlinear Dyn* 2020; 102(3): 1717–1731.
18. Yan X, Liu Y, Huang D, et al. A new approach to health condition identification of rolling bearing using hierarchical dispersion entropy and improved laplacian score. *Struct Health Monit* 2021; 20(3): 1169–1195.
19. Yan R and Gao RX. Approximate entropy as a diagnostic tool for machine health monitoring. *Mech Syst Signal Process* 2007; 21(2): 824–839.
20. Zhang L, Xiong G, Liu H, et al. An intelligent fault diagnosis method based on multiscale entropy and SVMs. In: Yu W, He H and Zhang N (eds.) *Advances in neural networks – ISNN 2009, 6th international symposium on neural networks, ISNN 2009, Wuhan, China, 26–29 May 2009 Proceedings, Part III*. Heidelberg: Springer, 2009, pp. 724–732.
21. Zheng J, Pan H and Cheng J. Rolling bearing fault detection and diagnosis based on composite multiscale fuzzy entropy and ensemble support vector machines. *Mech Syst Signal Process* 2017; 85: 746–759.
22. Zheng J, Cheng J and Yang Y. A rolling bearing fault diagnosis approach based on lcd and fuzzy entropy. *Mech Mach Theory* 2013; 70: 441–453.
23. Cheng G, Chen X, Li H, et al. Study on planetary gear fault diagnosis based on entropy feature fusion of

- ensemble empirical mode decomposition. *Measurement* 2016; 91: 140–154.
- 24. Li Y, Xu M, Wei Y, et al. A new rolling bearing fault diagnosis method based on multiscale permutation entropy and improved support vector machine based binary tree. *Measurement* 2016; 77: 80–94.
  - 25. Xu Z, Zhang H, Liu J, et al. A research on maximum symbolic entropy from intrinsic mode function and its application in fault diagnosis. *Math Probl Eng* 2017; 2017.
  - 26. Zhou R, Wang X, Wan J, et al. Edm-fuzzy: an euclidean distance based multiscale fuzzy entropy technology for diagnosing faults of industrial systems. *IEEE Trans Ind Inf* 2020; 17(6): 4046–4054.
  - 27. Rajagopalan V and Ray A. Symbolic time series analysis via wavelet-based partitioning. *Signal Process* 2006; 86(11): 3309–3320.
  - 28. Jiang Y, Peng CK and Xu Y. Hierarchical entropy analysis for biological signals. *J Comput Appl Math* 2011; 236(5): 728–742.
  - 29. Zhang X, Liang Y, Zhou J, et al. A novel bearing fault diagnosis model integrated permutation entropy, ensemble empirical mode decomposition and optimized SVM. *Measurement* 2015; 69: 164–179.
  - 30. Liang XH, Liu ZL, Pan J, et al. Spur gear tooth pitting propagation assessment using model-based analysis. *Chin J Mech Eng* 2017; 30(6): 1369–1382.
  - 31. Pan YH, Wang YH, Liang SF, et al. Fast computation of sample entropy and approximate entropy in biomedicine. *Comput Methods Programs Biomed* 2011; 104(3): 382–396.
  - 32. Rostaghi M and Azami H. Dispersion entropy: a measure for time-series analysis. *IEEE Signal Process Lett* 2016; 23(5): 610–614.
  - 33. Hsu CW, Chang CC, Lin CJ, et al. A practical guide to support vector classification, 2003.
  - 34. Chen HL, Yang B, Liu J, et al. A support vector machine classifier with rough set-based feature selection for breast cancer diagnosis. *Expert Syst Appl* 2011; 38(7): 9014–9022.